Evaluation of image reconstruction methods for 123I-MIBG-SPECT: a rank-order study.

Söderberg, Marcus; Mattsson, Sören; Oddstig, Jenny; Uusijärvi, Helena; Valind, Sven; Thorsson, Ola; Garpered, Sabine; Prautzsch, Tilmann; Tischenko, Oleg; Leide Svegborn, Sigrid

Published in:
Acta Radiologica

DOI:
10.1258/ar.2012.120078

2012

Evaluation of image reconstruction methods for ^{123}I-MIBG-SPECT: a rank-order study

Marcus Söderberg[1], Sören Mattsson[1], Jenny Oddstig[1], Helena Uusijärvi-Lizana[1], Sven Valind[2], Ola Thorsson[2], Sabine Garpered[2], Tilmann Prautzsch[3], Oleg Tischenko[4] and Sigrid Leide-Svegborn[1]

[1] Medical Radiation Physics, Department of Clinical Sciences Malmö, Lund University, Skåne University Hospital, SE-205 02 Malmö, Sweden
[2] Department of Clinical Physiology, Skåne University Hospital, SE-205 02 Malmö, Sweden
[3] Scivis wissenschaftlice Bildverarbeitung GmbH, GE-370 85 Göttingen, Germany
[4] Research Unit Medical Radiation Physics and Diagnostics (AMSD), Helmholtz Zentrum Muenchen – German Research Center for Environmental Health, Ingolstaedter Landstrasse 1, GE-857 64 Neuherberg, Germany

Corresponding author:
Marcus Söderberg
Medical Radiation Physics
Skåne University Hospital, Malmö
SE-205 02 Malmö
SWEDEN
Phone: +46 40 33 86 51
Fax: +46 40 96 31 85
E-mail: marcus.soderberg@med.lu.se

Background: There is an opportunity to improve the image quality and lesion detectability in single photon emission computed tomography (SPECT) by choosing an appropriate reconstruction method and optimal parameters for the reconstruction.

Purpose: To optimize the use of the Flash 3D reconstruction algorithm in terms of equivalent iteration (EI) number (number of subsets times the number of iterations) and to compare with two recently developed reconstruction algorithms ReSPECT and orthogonal polynomial expansion on disc (OPED) for application on ^{123}I-metaiodobenzylguanidine (MIBG)-SPECT.

Material and Methods: Eleven adult patients underwent SPECT 4 h and 14 patients 24 h after injection of approximately 200 MBq ^{123}I-MIBG using a Siemens Symbia T6 SPECT/CT. Images were reconstructed from raw data using the Flash 3D algorithm at eight different EI numbers. The images were ranked by three experienced nuclear medicine physicians according to their overall impression of the image quality. The obtained optimal images were then compared in one further visual comparison with images reconstructed using the ReSPECT and OPED algorithms.

Results: The optimal EI number for Flash 3D was determined to be 32 for acquisition 4 h and 24 h after injection. The average rank order (best first) for the different reconstructions for acquisition after 4 h was: Flash $3D_{32}$ > ReSPECT > Flash $3D_{64}$ > OPED, and after 24 h: Flash $3D_{16}$ > ReSPECT > Flash $3D_{32}$ > OPED. A fair level of interobserver agreement concerning optimal EI number and reconstruction algorithm was obtained, which may be explained by the different individual preferences of what is appropriate image quality.

Conclusion: Using Siemens Symbia T6 SPECT/CT and specified acquisition parameters, Flash $3D_{32}$ (4 h) and Flash $3D_{16}$ (24 h), followed by ReSPECT, were assessed to be the preferable reconstruction algorithms in visual assessment of ^{123}I-MIBG images.

Keywords: SPECT, image reconstruction, iterative method, analytic method, human observer.

Single photon emission computed tomography (SPECT) images are reconstructed from projection data acquired using rotating gamma cameras. The technique is based on either analytical or iterative methods (1). Historically, filtered back projection (FBP) has been the main method of reconstruction of SPECT images, but in recent years FBP has more and more been replaced by iterative algorithms (2). The reason for this is the computational power available today and the possibility to model the emission and detection process better. In addition, improved compensation for image-degrading effects such as attenuation, scatter, and variation of spatial resolution with distance between the collimator and the patient, can be included in the reconstruction process (3, 4).

Nowadays, several different iterative reconstruction techniques are available, but the most well-known is the maximum likelihood expectation maximization (5, 6) and its accelerated version: ordered subsets expectation maximization (OSEM) (7). For the OSEM category of iterative reconstruction algorithms, the projection data is grouped into subsets. One iteration is completed when all of the subsets have been processed. The number of subsets determines the reconstruction speed. The higher value the faster the reconstruction will be performed. A trade-off exists between contrast/resolution and noise as the number of subsets times the number of iterations (equivalent iterations; EI) increases. Noise increases as the number of subsets and iterations increases and the effect is additive; thus, it is possible to define the EI (8). The convergence speed is dependent on the size of the objects and the total number of counts (4, 9). Noise amplification can be avoided by early termination of the algorithm (using fewer EI) or by smoothing the images with a reconstruction filter (10). The drawback is the loss of spatial resolution.

Various studies have shown improvements in image quality and lesion detectability by optimizing the number of EI and choosing an appropriate reconstruction method by doing phantom measurements, as well as human observer studies (11-14). However, the optimal number of EI and reconstruction method is dependent on the specific situation and needs to be optimized for the specific clinical task. Receiver operating characteristic (ROC) studies or derivatives thereof are widely used in medical X-ray imaging to define differences in imaging procedures, but ROC studies are time-consuming, require a large patient cohort with normal and pathological subjects, and the truth needs to be known for each case. No current image quality criteria are established for nuclear medicine examinations as there are for X-ray images. However, if the diagnostic performances are comparable or the differences are small, a side-by-side review (rank-order study) may be useful (15, 16).

The purpose of this study was to optimize the use of the Flash 3D (Siemens Medical Solutions, Forchheim, Germany) reconstruction algorithm in terms of the number of EI and to compare with two recently developed reconstruction algorithms ReSPECT (Scivis GmbH, Göttingen, Germany) and orthogonal polynomial expansion on disc (OPED) for application on ^{123}I-metaiodobenzylguanidine (MIBG)-SPECT. A secondary purpose was to evaluate the potential for recently developed viewer software to be used for visual assessment studies in nuclear medicine.

Material and Methods

Acquisition process

Eleven patients (7 male and 4 female patients, mean age 57 years, age range 23-84 years, 3 pathologically positive) underwent SPECT 4 h after intravenous injection of approximately 200 MBq ^{123}I-MIBG and 14 patients (8 male and 6 female patients; mean age 62 years, age range 37-84 years, 4 pathologically positive) 24 h post-injection (p.i.). Ten patients were examined both after 4 h and 24 h. The patients included in the study were referred for the detection of the neuroendocrine tumors, such as pheochromocytomas or neuroblastomas, and their metastases. These tumors commonly occur in the abdomen or the adrenal glands. MIBG is a pharmaceutical with high uptake both in normal sympathetically innervated tissues (e.g. heart and salivary glands) and abnormal tissues (tumors of neuroendocrine origin associated with expression of neurohormone transporters) (17). ^{123}I-MIBG SPECT has good sensitivity and high specificity, both greater than 90% for the diagnosis of neuroblastoma and of pheochromocytoma (18).

Data were acquired by use of a Siemens Symbia T6 SPECT/CT system (Siemens Medical Solutions, Forchheim, Germany). The system is a combination of a dual-detector gamma camera and a 6-slice CT scanner. For all acquisitions the same protocol was used: 128×128 matrix, step and shoot, non-circular orbit (auto contour), 360° SPECT with 64 projections/detector and 30 s/frame. A low energy high resolution collimator was used and a symmetrical 15% wide energy window was centered at 159 keV. Additionally, one lower and one upper 15% wide energy window were used in order to perform the scatter correction.

Image reconstruction process

The reconstruction algorithms considered in this study were the iterative algorithms Flash 3D (19), ReSPECT (20), and the analytical algorithm OPED (21, 22).

The Flash 3D algorithm is based on the maximum likelihood reconstruction using ordered subsets. The algorithm includes the variation of resolution with source-detector distance in both the axial direction and the transverse plane (19). The raw data (projection images) were used to reconstruct images of eight different EI numbers: 8, 16, 32, 64, 80 (the department's default setting), 96, 128, and, 256 (Table 1). The post-filtering was a three-dimensional Gaussian filter with a full-width-at-half-maximum (FWHM) selected to be fixed at 8.4 mm. The higher value of FWHM, the smoother the image will be. With a too large value, the resolution and contrast are diminished. Attenuation correction (attenuation map from the CT scan) and scatter correction (triple-energy window scatter correction) were applied. The reconstructions were performed on the image processing workstation (Siemens Syngo) that is used routinely for SPECT reconstructions.

All images were also reconstructed by the iterative algorithm ReSPECT version 3 (20). ReSPECT is in principal based on maximum likelihood reconstruction using ordered subsets. The difference from OSEM is the way in which the correction factors are calculated. The correction factors are formed as a geometric mean value of each projection in one subset. Triple energy window scatter correction and attenuation correction by a homogeneous attenuation map were applied (μ/ρ=0.14 cm^2/g). A body contour map was determined automatically by scatter data. The algorithm includes depth-dependent resolution recovery in both the axial direction and the transverse plane. Noise reduction is done by transient algorithms specialized for regularization of Poisson noise. The reconstruction parameters (8 iterations and 32 subsets) for ReSPECT were taken from default values, which were optimized by experience from Scivis.

The reconstruction was also performed using OPED, which is based on the orthogonal polynomial expansion on the disc. By this method, the Radon data are decomposed in a special polynomial basis. The reconstruction is represented by a sum of components of this decomposition multiplied by the factors, which play the role of amplification (hard kernel) or suppression (soft kernel) of the higher order components (22). The OPED algorithm did not take into account attenuation and scatter corrections. Instead of applying the soft reconstruction kernel, the original hard reconstruction kernel was applied. However, before reconstruction with OPED, the raw data were denoised with a method described in (23).

Visual assessment

The SPECT images were interpreted by three experienced observers, all nuclear medicine physicians, by showing the image sets in the software package Scientific Visualizer (Scivis

GmbH, Göttingen, Germany). The Scientific Visualizer has been developed within the European Commission research project MADEIRA (Minimizing Activities and Doses by Enhancing Image quality in Radiopharmaceutical Administration) (24). The software was adapted for observer studies with the possibility of showing up to eight unlabeled image sets side-by-side. The SPECT data for each patient were presented side-by-side in sagittal, coronal, and transversal views and as a maximum intensity projection, in random order and unlabeled. The Scientific Visualizer ran on one of the department's regular workstations in a black and white scale and resolution set to 3280×2048. The observers were free to change the window level settings. No time limit was imposed on the observers´ evaluation.

Assessment 1. By showing images reconstructed at eight different EI numbers for Flash 3D (Fig. 1), the observers were asked to rank the three best image sets according to their overall impression of the image quality with regard to noise level, ability to discriminate uptakes in anatomical structures (e.g. liver, adrenal glands, kidneys, and spleen), introduction of artifacts, and if possible delineation of suspected pathology. The rank order was 1 (best) to 3 and all the remaining image sets obtained a rank order of 4. This procedure was performed for images acquired 4 h as well as 24 h after injection. The average distribution of image quality ranking for all observers was calculated for the different EI numbers. In addition, the rank order was obtained based on the calculated average of scores a given image set received, i.e. the lower the value the better the image quality.

Assessment 2. The two images considered to be the best in the Flash 3D series (as identified by their EI numbers) were compared with images reconstructed using the ReSPECT and OPED algorithms. The 4 image sets (Fig. 2) were displayed in the Scientific Visualizer and the observers were in the same manner as in the first visual assessment asked to rank the image sets according to their overall impression of the image quality. A rank order of 1 was again assigned to the image set judged to have the best overall image quality and a rank of 4 was assigned to the worst. The same procedure was performed for images acquired 4 h and 24 h after injection. The average distribution of image quality ranking for all observers was calculated for the different reconstruction methods. In addition, the rank order was obtained based on the calculated average of scores that a given image set received.

Statistical analysis

The interobserver agreement for multiple observers was determined using generalized kappa (κ) statistics (25). The κ can vary between -1.0 and 1.0. A κ of 1.0 indicates total agreement, whereas a κ of 0 means agreement by chance. The non-parametric Friedman test (26) was applied on the ranking data to evaluate if a statistically significant difference between the different number of EI and reconstruction algorithms could be established (α=0.05).

Results

The software Scientific Visualizer was found to be a user friendly system for quick opening and closing views, which makes it easy to compare different image sets. The processing time for the three reconstruction algorithms is comparable and is with today's available computational power not a limitation.

Assessment 1. Fig. 1 shows image sets acquired 4 h p.i. reconstructed at 8 different EI numbers using Flash 3D. As the number of EI increases, the contrast/resolution increases but simultaneously the image noise increases. The average distributions of image quality ranking for all observers to the different EI numbers are shown in Table 2. Table 3 contains the single observer ranking of overall image quality using different numbers of EI. The observers concluded that the optimal EI number was 32 for both 4 h and 24 h p.i. measurements, followed by 64 EI and 16 EI, respectively. The strength of the interobserver agreement was considered as fair (κ_{4h}=0.30, κ_{24h}=0.25). The Friedman test could not establish statistically significant difference between 32, 64, and 80 EI (4 h p.i.) and between 16 and 32 EI (24 h p.i.). However, there was a significant difference between 80 (the department's default setting) and 16 (24 h p.i.), and between 80 and 32 EI (24 h p.i.).

Assessment 2. Fig. 2 shows examples of the evaluated reconstruction methods. The average distributions of image quality ranking for all observers to the different reconstruction methods are shown in Table 4. The three observers average rank order of overall image quality using four different reconstruction methods for acquisitions 4 h p.i. were (best first): Flash $3D_{32}$ > ReSPECT > Flash $3D_{64}$ > OPED, and for acquisitions 24 h p.i.: Flash $3D_{16}$ > ReSPECT > Flash $3D_{32}$ > OPED (Table 5). Images reconstructed using the OPED algorithm were consequently by all observers selected as having worst image quality. Fig. 2C shows that the OPED reconstructed images were noisy and had streak-like artifacts. The strength of the interobserver agreement was considered as fair (κ_{4h}=0.27, κ_{24h}=0.25). The results from the Friedman tests are shown in Table 6. When considering the rating data for all observers, a significant difference between OPED and the remaining reconstruction algorithms was found for acquisitions after 4 h and 24 h. No statistically significant difference was found between Flash $3D_{32}$, Flash $3D_{64}$, and ReSPECT for acquisitions 4 h after injection. As well, no statistically significant difference was found between Flash $3D_{16}$ and ReSPECT for acquisitions 24 h after injection.

Discussion

There is an opportunity to improve the image quality and lesion detectability by choosing an appropriate reconstruction method and optimal reconstruction parameters (11-13). The optimal settings depend on, e.g., the clinical task, the target organs, the patient, and the preferences of the observer. Optimal reconstruction conditions and selection of algorithm need to be evaluated in each department for each system and clinical task since the type of detector, crystal size, correction methods etc. differ among the various systems. Fewer optimization trials in the form of observer performance studies have been performed for nuclear medicine imaging than for X-ray imaging. This study shows an example of how an optimization of this kind can be performed.

The most important parameters in iterative algorithms e.g. Flash 3D are the number of iterations, subsets, and the choice of reconstruction filter. In this study the EI number in the Flash 3D algorithm was varied from 8 to 256, resulting in eight kinds of reconstructed images. It was not possible to change the type of reconstruction filter. The filter FWHM was selected to be fixed at 8.4, aimed to minimize the number of variable parameters. This value is the department's default value. The ideal would be to perform an optimization study that incorporates all acquisition and reconstruction parameters, but that is very time consuming and require participation from physicians, technologists, and medical physicists.

The preferred EI number for Flash 3D in the first visual assessment was 32 for acquisitions 4 h and 24 h after injection. This is lower than the department's default setting of 80. Consequently the physicians preferred a more smoothed appearance. With higher EI number the contrast is improved but simultaneous the noise increases and reduces the achievable image quality. Due to the interobserver variability and the absence of significant difference between the two images considered being the best in the Flash 3D series (as identified by their EI numbers), both images were included for the second visual assessment. In the second assessment the preferred EI number for acquisitions 24 h p.i. were 16 instead of 32. When considering the ranking data from all observers, no statistically significant difference was found between 16 and 32 EI. However, the results indicate that we should lower the number of EI, especially for acquisitions 24 h after injection. Acquisitions 24 h p.i. compared to acquisitions 4 h after injection have a lower number of counts, resulting in more noise in the reconstructed images for higher EI. However, using too few EI is undesirable as the algorithm may not reach convergence everywhere in the reconstructed volume and small lesions will not be visible.

When considering data from all observers, Flash 3D was the preferred algorithm for acquisitions 4 h and 24 h after injection. However, analyzed individually one of the observers preferred ReSPECT for acquisitions 4 h after injection. The observer variability may be explained by differences in individual preferences of what is appropriate image quality. The fair interobserver reliability and the limited patient cohort explain the absence of statistically significant difference between Flash 3D and ReSPECT, when considering ranking data from all observers.

There is an opportunity to further improve the reconstructed images using ReSPECT by performing an optimization study of the reconstruction parameters, as performed for Flash 3D. It may also be possible to improve the image quality if CT based attenuation correction are implemented in ReSPECT. ReSPECT was evaluated in a previous study of parathyroid scanning with ^{99m}Tc-MIBI (27). The study demonstrated better image quality using ReSPECT compared to the algorithm HOSEM (Hermes Medical Solutions, Stockholm, Sweden).

OPED is a fast exact mathematical reconstruction method but its hard kernel version is not capable of dealing with high levels of noise as is found in SPECT images. This original version of OPED applied to the denoised raw data was ranked as worst image quality. The soft kernel is planned to be tested in the future. The reconstructed images were noisy and had streak-like artifacts due to the geometry of the SPECT data, and no attenuation and scatter correction are implemented yet. Due to the collimation in SPECT, the measured data are parallel in the classical sense, i.e. uniformly distributed projections with equi-spaced lateral sampling. OPED requires sinusoidal lateral sampling and consequently the SPECT data needs to be re-sampled. In general, OPED is more suitable for use in PET and CT (28).

Based on experience from the visual assessment, the Scientific Visualizer software will be further improved and implemented with settings such as linking the window level and slice orientation between the different image sets. The viewer has potential as a very useful tool in the framework of optimizing nuclear medicine imaging.

The results obtained in studies like this are specific for the system and parameter settings. The outcome might vary by the amount of radionuclide activity used, acquisition parameters, acquisition time, and examined body area. Another possible limitation is that the observers might have recognized and were familiar with the Flash 3D reconstructions. The primary selection of preferred EI number for Flash 3D in the first visual assessment could also have formed a bias in its favor. To reduce this source of bias, the second assessment was carried out a couple of weeks after the first assessment.

The result of this rank-order study gives an indication of preferred reconstruction parameters and algorithms, which need to be further investigated with a larger patient cohort. The impact on diagnostic performance was not investigated, and there are variations in patient size, shape, and uptake affinity for the radiopharmaceutical that may influence the result. However, our results are useful for future optimization of reconstruction methods and parameter settings.

In conclusion, using Siemens Symbia T6 SPECT/CT and specified acquisition parameters, Flash $3D_{32}$ (4 h p.i.) and Flash $3D_{16}$ (24 h p.i.), followed by ReSPECT were assessed to be the preferable reconstruction algorithms in visual assessment of ^{123}I-MIBG images. In our department the number of EI has been reduced from 80 to 32.

Acknowledgements

The work was carried out within the Collaborative Project "MADEIRA" (www.madeira-project.eu), cofounded by the European Commission through EURATOM Seventh

Framework Programme (Grant Agreement FP7-212100). The authors would like to thank Dr. Gernot Ebel, Dr. Timo Aspelmeier, and Dr. Björn Thiel for support and adaptation with ReSPECT and the Scientific Visualizer.

References

1. Bruyant PP. Analytic and iterative reconstruction algorithms in SPECT. *J Nucl Med* 2002;**43**:1343-58

2. Vandenberghe S, D'Asseler Y, Van de Walle R, *et al*. Iterative reconstruction algorithms in nuclear medicine. *Comput Med Imaging Graph* 2001;**25**:105-11

3. Groch MW, Erwin WD. SPECT in the year 2000: basic principles. *J Nucl Med Technol* 2000;**28**:233-44

4. Hutton BF, Hudson HM, Beekman FJ. A clinical perspective of accelerated statistical reconstruction. *Eur J Nucl Med* 1997;**24**:797-808

5. Lange K, Carson R. EM reconstruction algorithms for emission and transmission tomography. *J Comput Assist Tomogr*. 1984;**8**:306-16

6. Shepp LA, Vardi Y. Maximum likelihood reconstruction for emission tomography. *IEEE Trans Med Imaging*. 1982;**1**:113-22.

7. Hudson HM, Larkin RS. Accelerated image reconstruction using ordered subsets of projection data. *IEEE Trans Med Imaging* 1994;**13**:601-9

8. Brambilla M, Cannillo B, Dominietto M, *et al*. Characterization of ordered-subsets expectation maximization with 3D post-reconstruction Gauss filtering and comparison with filtered backprojection in ^{99m}Tc SPECT. *Ann Nucl Med* 2005;**19**:75-82

9. Liow JS, Strother SC. The convergence of object dependent resolution in maximum likelihood based tomographic image reconstruction. *Phys Med Biol* 1993;**38**:55-70

10. Beekman FJ, Slijpen ET, Niessen WJ. Selection of task-dependent diffusion filters for the post-processing of SPECT images. *Phys Med Biol* 1998;**43**:1713-30

11. Gutman F, Gardin I, Delahaye N, *et al*. Optimisation of the OS-EM algorithm and comparison with FBP for image reconstruction on a dual-head camera: a phantom and a clinical ^{18}F-FDG study. *Eur J Nucl Med Mol Imaging* 2003;**30**:1510-9

12. Inoue K, Sato T, Kitamura H, *et al*. Improvement of the diagnostic accuracy of lymph node metastases of colorectal cancer in ^{18}F-FDG-PET/CT by optimizing the iteration number for the image reconstruction. *Ann Nucl Med* 2008;**22**:465-73

13. Koch W, Hamann C, Welsch J, *et al*. Is iterative reconstruction an alternative to filtered backprojection in routine processing of dopamine transporter SPECT studies? *J Nucl Med* 2005;**46**:1804-11

14. Zeintl J, Vija AH, Chapman JT, *et al*. Quantifying the Effects of Acquisition Parameters in Cardiac SPECT Imaging and Comparison with Visual Observers. *2006 IEEE Nuclear Science Symposium Conference Record* 2006;**6**:3251-57

15. Good WF, Sumkin JH, Dash N, *et al*. Observer sensitivity to small differences: a multipoint rank-order experiment. *Am J Roentgenol* 1999;**173**:275-78

16. Towers JD, Holbert JM, Britton CA, *et al*. Multipoint rank-order study methodology: observer issues. *Invest Radiol* 2000;**35**:125-30

17. Vallabhajosula S, Nikolopoulou A. Radioiodinated metaiodobenzylguanidine (MIBG): radiochemistry, biology, and pharmacology. *Semin Nucl Med* 2011;**41**:324-33

18. Jacobson AF, Deng H, Lombard J, *et al*. ^{123}I-meta-iodobenzylguanidine scintigraphy for the detection of neuroblastoma and pheochromocytoma: results of a meta-analysis. *J Clin Endocrinol Metab* 2010;**95**:2596-606

19. Hawman E, Vija H, Daffach R, *et al*. Flash 3D technology Optimizing SPECT quality and accuracy. *Whitepaper Flash 3D*. Siemens Medical Solutions, 2003:1-6

20. Scivis GmbH. *ReSPECT - Technical description*. Scivis, 2006:1-27

21. Tischenko O, Xu Y, Hoeschen C. Main features of the tomographic reconstruction algorithm OPED. *Radiat Prot Dosimetry* 2010;**139**:204-7

22. Xu Y, Tischenko O, Hoeschen C. Image reconstruction by OPED algorithm with averaging. *Numer Algor* 2007;**45**:179-93

23. Tischenko O, Hoeschen C, Buhr E. Reduction of anatomical noise in medical X-ray images. *Radiat Prot Dosimetry* 2005;**114**:69-74

24. Hoeschen C, Mattsson S, Cantone MC, *et al*. Minimising activity and dose with enhanced image quality by radiopharmaceutical administrations. *Radiat Prot Dosimetry* 2010;**139**:250-3

25. Fleiss JL. Measuring nominal scale agreement among many raters. *Psychological Bulletin* 1971;**76**:378-82

26. Friedman M. The use of ranks to avoid the assumption of normality implicit in the analysis of variance. *Journal of the American Statistical Association* 1937;**32**:675-701

27. Van Hoorn R, Vriens D, Postema J, *et al*. Evaluation of the advanced ReSPECT image reconstruction software in a phantom model and in parathyroid scanning. *J Nucl Med* 2010;**51** (Supplement 2): 1352

28. Xu Y, Tischenko O, Hoeschen C. A new reconstruction algorithm for radon data. *Proc SPIE* 2006;**6142**:791-8

Table 1. The number of iterations and subsets that each equivalent iteration contains.

EI	Iterations	Subsets
8	2	4
16	4	4
32	4	8
64	8	8
80	10	8
96	12	8
128	8	16
256	8	32

Table 2. Distribution of image quality ranking as a function of rank and the number of equivalent iterations in the Flash 3D reconstruction. The table summarizes results for all observers. Each entry is the fraction of observers that assigned the actual rank to the specific equivalent iteration. The best three images were ranked 1-3 and all the remaining image sets obtained a rank order of 4.

Acquisition	Rank order	8	16	32	64	80	96	128	256
4 h	1	0.00	0.09	0.45	0.18	0.18	0.06	0.03	0.00
	2	0.00	0.03	0.21	0.48	0.18	0.06	0.03	0.00
	3	0.00	0.06	0.15	0.21	0.33	0.24	0.00	0.00
	4	1.00	0.82	0.18	0.12	0.30	0.64	0.94	1.00
24 h	1	0.19	0.26	0.50	0.02	0.02	0.00	0.00	0.00
	2	0.07	0.40	0.24	0.19	0.07	0.10	0.00	0.00
	3	0.05	0.07	0.24	0.43	0.10	0.12	0.00	0.00
	4	0.69	0.26	0.02	0.36	0.81	0.86	1.00	1.00

Table 3. Single observer ranking of overall image quality using the Flash 3D algorithm. Each entry in the table contains the equivalent iteration number that the observer assigned to a specific rank.

	4 h			24 h		
Observer	**Rank 1**	**Rank 2**	**Rank 3**	**Rank 1**	**Rank 2**	**Rank 3**
A	32/64		80	32	16	64
B	32	64	80	16	8	32
C	80	64	96	32	64	16
Average	32	64	80	32	16	64

Table 4. Distribution of image quality ranking as a function of the rank and the SPECT reconstruction method. Each entry is the fraction of observers that assigned the actual rank to the specific reconstruction method. The rank order was 1 (best) to 4.

Acquisition	Rank order	Flash $3D_{16}$	Flash $3D_{32}$	Flash $3D_{64}$	ReSPECT	OPED
4 h	1	-	0.39	0.21	0.39	0.00
	2	-	0.52	0.27	0.21	0.00
	3	-	0.09	0.52	0.39	0.00
	4	-	0.00	0.00	0.00	1.00
24 h	1	0.55	0.17	-	0.29	0.00
	2	0.36	0.33	-	0.31	0.00
	3	0.10	0.50	-	0.40	0.00
	4	0.00	0.00	-	0.00	1.00

Table 5. Single observer ranking of overall image quality using Flash 3D, ReSPECT and OPED. Each entry in the table contains the reconstruction method that the observer assigned to a specific rank.

	4 h				24 h			
Observer	Rank 1	Rank 2	Rank 3	Rank 4	Rank 1	Rank 2	Rank 3	Rank 4
A	ReSPECT	Flash $3D_{32}$	Flash $3D_{64}$	OPED	Flash $3D_{16}$	ReSPECT	Flash $3D_{32}$	OPED
B	Flash $3D_{32}$	Flash $3D_{64}$/ReSPECT		OPED	Flash $3D_{16}$	Flash $3D_{32}$	ReSPECT	OPED
C	Flash $3D_{64}$	Flash $3D_{32}$	ReSPECT	OPED	Flash $3D_{32}$	Flash $3D_{16}$	ReSPECT	OPED
Average	Flash $3D_{32}$	ReSPECT	Flash $3D_{64}$	OPED	Flash $3D_{16}$	ReSPECT	Flash $3D_{32}$	OPED

Table 6. Results of the Friedman tests (27). If a statistically significant difference was established between two reconstruction algorithms, it is indicated for each observer A, B, and C, respectively. The shaded areas indicate that a statistically significant difference was established based on the ranking data for all observers.

	4 h				24 h		
	Flash $3D_{32}$	Flash $3D_{64}$	ReSPECT		Flash $3D_{16}$	Flash $3D_{32}$	ReSPECT
OPED	A, B, C	B, C	A, B, C	**OPED**	A, B, C	B, C	A, B, C
ReSPECT		A		**ReSPECT**	B	A	
Flash $3D_{64}$				**Flash $3D_{32}$**	A		

Fig. 1. Image sets acquired 4 h after the injection of approximately 200 MBq ^{123}I-MIBG and reconstructed at eight different EI numbers for Flash 3D: (A) 8, (B) 96, (C) 256, (D) 80, (E) 64, (F) 32, (G) 128 and (H) 16.

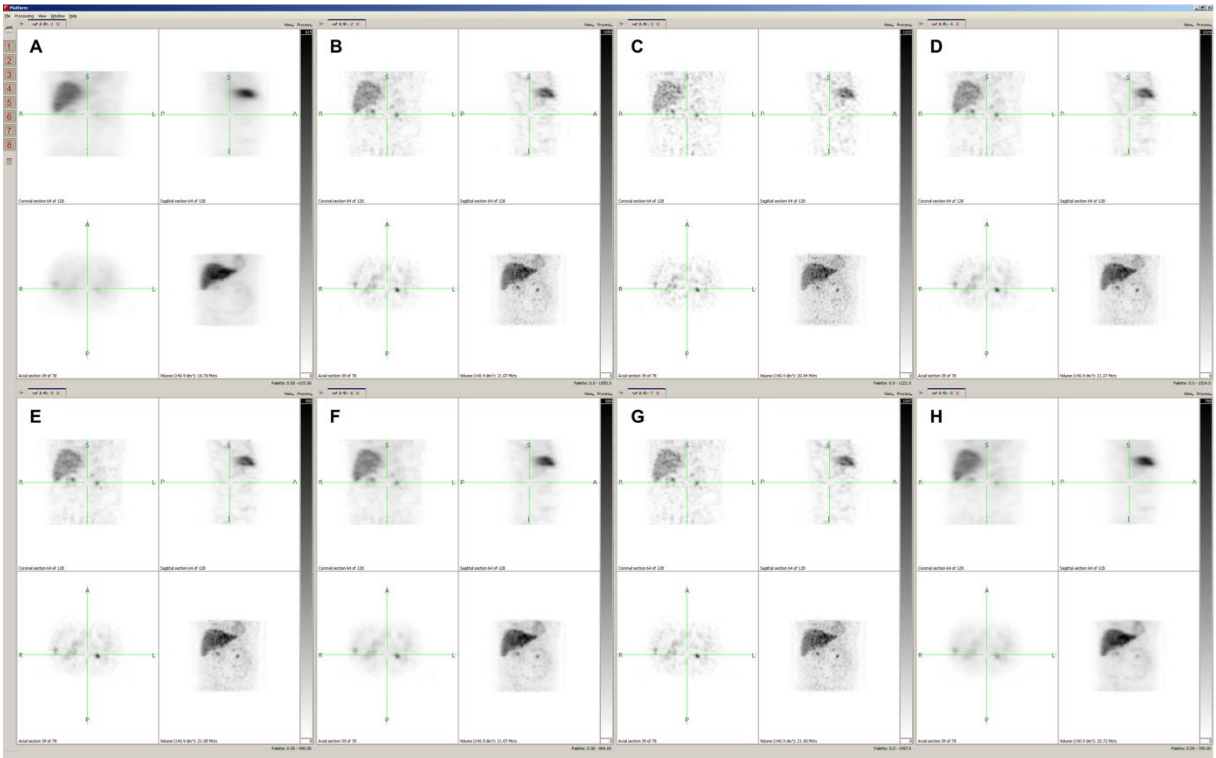

Fig. 2. Image sets acquired 4 h after the injection of approximately 200 MBq ^{123}I-MIBG and reconstructed using different reconstruction methods: (A) ReSPECT, (B) Flash $3D_{64}$, (C) OPED and (D) Flash $3D_{32}$.